

Unidentified Infrared Emission Bands in the Diffuse Interstellar Medium¹

Kin-Wing Chan^{2,3}, T. L. Roellig², T. Onaka⁴, M. Mizutani⁴, K. Okumura⁵, I. Yamamura⁶, T. Tanabé⁷, H. Shibai⁸, T. Nakagawa⁶, and H. Okuda⁹

ABSTRACT

Using the Mid-Infrared Spectrometer on board the Infrared Telescope in Space and the low-resolution grating spectrometer (PHT-S) on board the Infrared Space Observatory, we obtained 820 mid-infrared (5 to 12 μm) spectra of the diffuse interstellar medium (DIM) in the Galactic center, W51, and Carina Nebula regions. These spectra indicate that the emission is dominated by the unidentified infrared (UIR) emission bands at 6.2, 7.7, 8.6, and 11.2 μm . The relative band intensities (6.2/7.7 μm , 8.6/7.7 μm , and 11.2/7.7 μm) were derived from these spectra, and no systematic variation in these ratios was found in our observed regions, in spite of the fact that the incident radiation intensity differs by a factor of 1500. Comparing our results with the polycyclic aromatic hydrocarbons (PAHs) model for the UIR band carriers, PAHs in the DIM have no systematic variation in their size distribution, their degree of dehydrogenation is independent of the strength of UV radiation field, and they are mostly ionized. The finding that PAHs in the DIM with low UV radiation field strength are mostly ionized is incompatible with past theoretical studies, in which a large fraction of neutral PAHs is predicted in this kind of environment. A plausible resolution of this discrepancy is that the recombination coefficients for electron and large PAH positive ion are by at least an order of magnitude less than those adopted in past theoretical studies. Because of the very low population of neutral state molecules,

¹Based on observations with ISO, an ESA project with instruments funded by ESA member states (especially the PI countries France, Germany, the Netherlands, and the United Kingdom) and with the participation of ISAS and NASA.

²NASA Ames Research Center, MS 245-6, Moffett Field, CA 94035-1000

³present address: Department of Astronomy, University of Tokyo, Bunkyo-ku, Tokyo 113-0033, Japan, kwc@astron.s.u-tokyo.ac.jp

⁴Department of Astronomy, University of Tokyo, Bunkyo-ku, Tokyo 113-0033, Japan

⁵Communications Research Laboratory, Koganei, Tokyo 184-8795, Japan

⁶Institute of Space and Astronautical Science, Sagami-hara, Kanagawa 229-8510, Japan

⁷Institute of Astronomy, University of Tokyo, Mitaka, Tokyo 181-8588, Japan

⁸Department of Physics, Nagoya University, Chikusa-ku, Nagoya 464-8602, Japan

⁹Gunma Astronomical Observatory, Gunma 377-0702, Japan

photoelectric emission from interstellar PAHs is probably not the dominant source of heating of the diffuse interstellar gas. The present results imply constant physical and chemical properties of the carriers of the UIR emission bands in the DIM covering the central and disk regions of the Galaxy, which could help in the identification of the carriers.

Subject headings: dust extinction—infrared: ISM: lines and bands

1. Introduction

The so-called unidentified infrared (UIR) emission bands include features that always occur together at 3.3, 6.2, 7.7, 8.6, 11.2, and 12.7 μm . Since the first detection of the 11.2 μm band by Gillett, Forrest, & Merrill (1973) in planetary nebulae, the UIR bands have been observed in a variety of sources (see Tokunaga 1997 for a recent review). Puget, Léger, & Boulanger (1985) have proposed that the excess *IRAS* 12 μm emission observed in the Galactic diffuse clouds (Boulanger, Baud, & van Albada 1985) can be attributed to the longer wavelength UIR emission bands. The detection of these emission bands in the diffuse interstellar medium (DIM) has strongly favored this explanation of the excess *IRAS* 12 μm emission in the Galaxy (see Onaka et al. 1996; Mattila et al. 1996 and references therein). The consequences of this hypothesis imply that the carriers of the UIR bands play an important role in the energy balance and chemical processes in the Galaxy.

To date there is still no definite identification of the carriers of the UIR emission bands. Several carriers have been proposed: polycyclic aromatic hydrocarbons (PAHs; Léger & Puget 1984; Allamandola, Tielens, & Barker 1985), quenched carbonaceous composite (QCC; Sakata et al. 1984), hydrogenated amorphous carbon (HAC; Duley & Williams 1981), and coal grains (Papoular et al. 1989). Among these the PAHs are the most thoroughly studied in both theoretical and laboratory studies, and therefore one can make quantitative comparison between the observations and model calculations. For example, one can compare the observed spectra with those of PAH spectra measured in the laboratory. One can also compare the observed relative UIR band intensities in different UV radiation environments with those predicted by the PAHs model. In the PAHs model, changes in the degree of dehydrogenation and/or in the relative abundance of neutral and ionic PAHs can change the near- and mid-infrared band intensities (e.g., Jourdain de Muizon, d’Hendecourt, & Geballe 1990; Schutte, Tielens, & Allamandola 1993; Allamandola, Hudgins, & Sandford 1999).

The DIM is an ideal environment for testing the PAHs model. The properties of dust grains particular to their formation place should be averaged out and the stable species should be abundant there. Studies of the UIR emission bands in the DIM covering a wide range of UV radiation field strengths uniquely test the physical process operating on the interstellar PAHs. The UIR band emission in the DIM, however, is difficult to observe with ground-based warm telescopes, and some bands are strongly absorbed in the terrestrial atmosphere. High sensitivity space-borne observations are required for this study. In this paper we present results from a large sample of mid-infrared

spectrophotometric observations in the DIM which were obtained from the Infrared Telescope in Space (IRTS) and the Infrared Space Observatory (ISO). We discuss discrepancies between the present results and the predictions from the PAHs model.

2. Observations

The Mid-Infrared Spectrometer (MIRS) was one of the four science focal-plane instruments that flew aboard the orbiting IRTS. The IRTS was the first Japanese infrared space-borne telescope developed and operated in collaboration with NASA. It was launched on 1995 March 18 and surveyed $\sim 7\%$ of the sky over the course of its 26-day mission life (Murakami et al. 1996). The MIRS had an aperture size of $8' \times 8'$ and operated over a wavelength range of 4.5 to 11.7 μm with a resolution of $\Delta\lambda = 0.23$ to 0.36 μm (Roellig et al. 1994). During the course of its mission, the MIRS observed part of the Galactic center and W51 regions and we present here the DIM data at $l = 0^\circ$ to -12° with $|b| \leq 2^\circ$ and $l = 45^\circ$ to 51° with $|b| \leq 2^\circ$. The uncertainty of the absolute calibration is about 10% (see Tanabé et al. 1997 for details of the MIRS calibration). The selected regions for this study did not include bright *IRAS* point sources, and the zodiacal background emission has been subtracted. To subtract the zodiacal background, we extracted background spectra that were observed by the MIRS at regions a few degrees of galactic latitude and longitude away from the selected regions. The uncertainties in the zodiacal emission subtraction in our selected regions are many times lower than the galactic plane emission there. The total far-infrared intensity, *FIR*, and optical depth at 100 μm , $\tau_{100\mu\text{m}}$, at each position have been obtained from Okumura (1998), who used the 155 μm continuum fluxes from the Far-Infrared Line Mapper (FILM) on board the IRTS (Okumura et al. 1996) and the *IRAS* Sky Survey Atlas (ISSA; Wheelock et al. 1994) 100 μm fluxes to derive those values (see also Okumura et al. 1999). The dust temperature, T , and $\tau_{100\mu\text{m}}$ were derived from a modified blackbody (a blackbody multiplied by a λ^{-2} dust emissivity law) fit to the 100 and 155 μm fluxes. The *FIR* is estimated as

$$FIR = \tau_{100\mu\text{m}} \int_0^\infty [100\mu\text{m}/\lambda(\mu\text{m})]^2 B_\lambda(T) d\lambda, \quad (1)$$

where $B_\lambda(T)$ is the Planck function and λ is the wavelength in μm . The FILM has a beam size of $8' \times 13'$ and the ISSA 100 μm fluxes have been smoothed into a $12'$ resolution with a $4'$ bin. The *FIR* in our selected regions has a range of 4×10^{-6} to 1000×10^{-6} $\text{W m}^{-2} \text{sr}^{-1}$. Following Okumura (1998) we estimate the incident radiation intensity in units of the interstellar radiation field of the solar neighborhood ($= 1.6 \times 10^{-6}$ W m^{-2} , Habing 1968), G_0 , from the *FIR* as

$$G_0 = \frac{4\pi FIR}{1.6 \times 10^{-6} \langle \tau_{abs} \rangle}, \quad (2)$$

where $\langle \tau_{abs} \rangle$ is the absorption optical depth averaged over the incident radiation field. Since G_0 defined here covers a wavelength range from UV to visible, it should be larger than the G_0 defined by Habing (1968), in which the incident intensity includes only the UV range.

In addition to the MIRS data, we also included data of the observations of the Carina Nebula region with the low-resolution spectrometer (PHT-S) and long-wavelength spectrometer (LWS) on board the ISO (Kessler et al. 1996). The ISO observations were made in a two-dimensional raster mode with a spacing of $3'$ for a rectangular area of $40' \times 20'$ centered at $l = 287^\circ.25$ and $b = -0.6^\circ$ (see Mizutani, Onaka, & Shibai 1999 for details of the observation). The observed region included the DIM and molecular clouds in the Carina Nebula. The PHT-S had an aperture size of $24'' \times 24''$ and operated over a wavelength range of 2.5 to $11.6 \mu\text{m}$ with a spectral resolution of about 90 (Lemke et al. 1996). Only the data between 5.7 and $11.6 \mu\text{m}$ is used in the present study. The PHT-S data were reduced by PIA version 8.1. Special care was taken for the effects after cosmic ray hits in the raster scan mode and the data affected by the cosmic ray hit were removed. The LWS observations were made in the full grating scanning mode (LW01) for 45 to $170 \mu\text{m}$ with a spectral resolution of about 200 (Clegg et al. 1996). The LWS beam size varies with detector, ranging from $60''$ to $84''$ FWHM (Gry 2000). The pipeline version 7 data products were used for the LWS data. The data were defringed by software developed based on the subroutine in the ISO Spectral Analysis Package (ISAP¹⁰). The gaps between the detectors were corrected by scaling the fluxes relative to the SW2 detector such that the adjacent detector signals were connected smoothly. All the observed positions were quite bright in the far-infrared. Therefore the detector dark current was insignificant and we attributed the gaps mostly to uncertainties in the response or differences in the aperture size of each detector. The correction does not exceed 20% and it does not affect the conclusions of this paper. Because the LWS spectra are calibrated against a point-like source, a beam-size correction was needed for observations of diffuse sources. The values given in Table 7.1 of the LWS Data Users Manual (Trams et al. 1998) were fitted to a quadratic function of the wavelength and the beam-size correction was made based on the function. The resultant spectra can be well fitted with a blackbody times a λ^{-1} emissivity. The values of FIR and G_0 were derived in a similar manner as for the ISSA/FILM data, though we used a λ^{-1} emissivity in the LWS data instead of a λ^{-2} emissivity. The beam-size correction affects the FIR by about 30% and hence G_0 by the same amount. The absolute values of FIR and G_0 may have large uncertainties owing to this correction and the uncertainty in the beam size (Burgdorf et al. 1997), while their relative scale was less affected and the relative order was not affected at all. The following discussions are made mostly on an order-of-magnitude basis and are not affected by these uncertainties. Taking the value of $\langle \tau_{abs} \rangle / \tau_{100\mu m} = 700$ (Draine & Lee 1984), the range of FIR in our selected regions yields values for G_0 of 3 to 4500. Total of 820 spectra were obtained for the following analysis.

¹⁰The ISO Spectral Analysis Package (ISAP) is a joint development by the LWS and SWS Instrument Teams and Data Centers. Contributing institutes are CESR, IAS, IPAC, MPE, RAL and SRON.

3. Results

Since the extinction towards the Galactic center and W51 regions is high even in mid-infrared wavelengths, extinction corrections of the spectra of these regions were necessary. At each of the observed positions, we used the derived $\tau_{100\mu m}$ and then employed the extinction law of Mathis (1990) to correct for interstellar extinction. The extinction corrected UIR band ratios, which will be discussed later, show values by a few percent to 20% different compared to those without the extinction correction. The visual extinction towards the Carina Nebula is low, with an average A_V of ~ 0.5 (Feinstein, Marraco, & Muzzio 1973). Similar low extinction values have been obtained from the derived $\tau_{100\mu m}$. The low visual extinction corresponds to less than a 1% difference between the extinction-corrected and uncorrected UIR band ratios, and therefore, no extinction correction has been applied to the Carina Nebula spectra.

For all of the observed positions, the MIRS and PHT-S detected four UIR bands at 6.2, 7.7, 8.6, and 11.2 μm . These observed mid-infrared spectra are similar in shape to those taken in the DIM around the W51 region (Onaka et al. 1996). Figure 1 shows some of the observed spectra in our three observed regions, and they are quite similar to each other even though they are observed in different parts of the Galaxy. The intensities of the 6.2, 8.6, and 11.2 μm band relative to those of the 7.7 μm band have been derived. Following Onaka et al. (1996), we drew a straight line between the edges of the emission features for each band where the flux was assumed to come predominantly from the continuum and integrated the flux above the lines as a measure of the band intensities (see Figure 1). For the MIRS spectra, the wavelength points selected as continuum are 5.95 and 6.64 μm , 7.09 and 8.22 μm , 8.22 and 9.12 μm , and 10.91 and 11.59 μm for the 6.2, 7.7, 8.6, and 11.2 μm feature bands, respectively. Similar wavelength points were selected in the PHT-S spectra.

Figure 2 shows the plot of the relative band intensities of the 6.2/7.7 μm , 8.6/7.7 μm , and 11.2/7.7 μm vs. G_0 . No systematic variation is found in those figures. The ratios do not show any increasing or decreasing trend with G_0 . The average relative band intensity ratios for the 6.2/7.7 μm , 8.6/7.7 μm , and 11.2/7.7 μm are 0.39, 0.24, and 0.40, respectively.

4. Discussion

The finding of no systematic variation in the UIR band ratios over a wide range of G_0 has also been reported in the interstellar medium (Boulanger et al. 1998; Uchida et al. 2000). Uchida et al. (2000) studied a sample of reflection nebulae and found that the UIR band ratios show no systematic variation over a range of hardness and strength of UV radiation fields ($T_{eff} = 6800$ to 22,000 K and $G_0 = 40$ to 1800). On the other hand, variations of the UIR band ratio have been observed in environments covering a wide range of physical and chemical conditions (e.g., Cohen et al. 1986; Bregman et al. 1994, 1995; Joblin et al. 1996; Roelfsema et al. 1996; Cesarsky et al. 1996; Lu 1998; Mattila, Lehtinen, & Lemke 1999). Since the present results together with the results of Uchida et al. (2000) suggest that the UIR band ratios are independent of the hardness and strength

of the UV radiation field, there must be some other parameters that contribute to the variation in the strength of the UIR band emission in the interstellar medium. A plausible explanation of these conflicting results is that the physical and chemical properties of the carriers of the UIR bands vary in environments where the carriers have just formed or where the chemical abundances are different. For PAHs model, the newly formed PAHs consist of a large amount of unstable molecules, which have very different band ratios compared with those of the more stable ones (Allamandola et al. 1999). For QCC and coal models, the available oxygen can change the oxidization of these materials, which changes their emission band ratios (Sakata et al. 1987; Papoular et al. 1989). Further studies are needed to elucidate the cause of the variations. Because different authors use different continuum baselines in the derivation of the UIR band intensity, quantitative comparison of the derived value of the UIR band ratios in a certain UV radiation field strength is difficult. The variations found by those past studies could be within the range of the present data shown in Figure 2, but they are not correlated with G_0 in the present results.

The PAHs model we will test is a general model without specifying its composition. In the PAHs model the 6.2 and 7.7 μm bands arise from the C–C stretching vibrations of the PAH molecules and the 8.6 and 11.2 μm bands arise from the C–H in-plane and out-of-plane bending vibrations, respectively. According to the proposed emission mechanisms, such as infrared fluorescence, the relative UIR band ratios should not change with G_0 . Any change in the band ratios must be associated with changes in the ionization, dehydrogenation, or size of the carriers. For instance, neutral PAHs show quite weak 6.2, 7.7, and 8.6 μm bands compared to the observed interstellar spectra, while these bands are enhanced significantly in ionized PAHs (Allamandola et al. 1999 and references therein). The observed PAH bands can be used to derive the physical and chemical properties of PAH molecules in the observed astronomical environments.

The 6.2/7.7 μm band ratio displays variations among and within sources covering a wide range of physical and chemical properties (Cohen et al. 1986; Bregman et al. 1995; Roelfsema et al. 1996; Lu 1998; Mattila et al. 1999). The variations could be due to the changes of mean energy of the incident UV photons or size of PAHs. Figure 2a shows that there is no systematic variation in the 6.2/7.7 μm band ratio with G_0 . The difference in excitation energy between the 6.2 and 7.7 μm bands is small and the variation in the spectrum of the diffuse interstellar radiation field should not be large enough to change this band ratio. Therefore, PAHs in the DIM do not have a systematic variation in their size distribution.

The 8.6/7.7 μm band ratio can be used as an indicator of the degree of dehydrogenation of PAHs. The ratio decreases if the degree of dehydrogenation of the PAHs increases (e.g., Jourdain de Muizon et al. 1990; Schutte et al. 1993). By comparing the calculated results to the observed PAH emission bands in the Orion Bar region, Schutte et al. (1993) concluded that the interstellar PAHs are almost fully hydrogenated. Allamandola, Tielens, & Barker (1989) also concluded that, based on the calculated hydrogen loss rates and rehydrogenation rates of PAHs, the interstellar PAHs are fully hydrogenated if the PAHs are larger than 25 to 30 carbon atoms. The present finding suggests that the degree of dehydrogenation of PAHs in the DIM is independent of G_0 over

$G_0 = 3$ to 4500.

The ionization state of PAHs can be deduced from the relative intensities between the 7.7 and 11.2 μm band emission. For neutral PAHs the intensity of the 11.2 μm band emission is higher than those of the 7.7 μm band emission and vice versa for ionized PAHs (Schutte et al. 1993; Allamandola et al. 1999). A study of the spacing between the 6.2 and 7.7 μm band emission suggested that the interstellar PAHs have sizes of 50 to 80 carbon atoms (Hudgins & Allamandola 1999). Theoretical studies showed that a large fraction of neutral PAHs with 50 to 80 carbon atoms should exist in the DIM where G_0 is ~ 1 , and they are almost completely positively ionized in reflection nebulae and photodissociation regions where G_0 is $\sim 10^5$ (Omont 1986; d’Hendecourt & Léger 1987; Verstraete et al. 1990; Bakes & Tielens 1994; Dartois & d’Hendecourt 1997). Since the exact composition of PAHs existing in space is still unknown, it is difficult to estimate their relative band ratios in neutral and ionized interstellar PAHs. We roughly estimate these ratios in the following by simple scaling.

Schutte et al. (1993) found that the 11.2/7.7 μm band ratio increases by a factor of 5.2 when they compared this band ratio in their standard model with those in the neutral PAHs model. Their standard model gave a good fit to the interstellar UIR bands emission in the Orion Bar, where the PAHs are suggested to be totally ionized in a recent study by Allamandola et al. (1999). Therefore, we first assume that the 11.2/7.7 μm ratio increases by a factor of 5.2 when the interstellar PAHs change from 100% ionized to 100% neutral. Then, we use the spectrum of the Orion Bar to derive the 11.2/7.7 μm band ratio for interstellar PAHs with 100% ionized, and finally multiply this derived band ratio by the factor 5.2 to obtain the 11.2/7.7 μm band ratio for interstellar PAHs of 100% neutral. By using the same baselines in the derivations of our UIR band intensities, we find that the Orion Bar emission shown in Allamandola et al. (1999) has a 11.2/7.7 μm band ratio of 0.3. Therefore, the 11.2/7.7 μm band ratio is assumed to have a value of 1.5 for 100% neutral PAHs in the interstellar medium. In figure 2c, almost all of the 11.2/7.7 μm ratios are less than 1.5, which suggests that only a small fraction of PAHs are neutral in the DIM. Assuming the value of the band ratio can be scaled linearly between 0.3 (100% ionized) and 1.5 (0% ionized) with the ionization fraction of interstellar PAHs, figure 2c suggests that the ionization fraction of PAHs in the DIM is between 60% and 100%, with a mean value of 90%, and that the degree of ionization shows no systematic variation in the range of $G_0 = 3$ to 4500. The finding here is incompatible with those previous theoretical studies, and this discrepancy can be resolved if the recombination coefficients for electron-PAH ion interactions are much lower than those adopted in the previous theoretical studies.

The ionization fraction, $f(+)$, of PAHs depends on the photoionization rate for the neutral PAHs, R_{ion} , and the recombination rate for electron and PAH positive ion, R_{rec} , and can be written as

$$f(+) = \frac{R_{ion}}{R_{ion} + R_{rec}}. \quad (3)$$

The photoionization rate for neutral PAHs is proportional to the incident UV radiation intensity and the photoionization cross-section of the neutral PAHs. Based on the past laboratory measurement of the photoionization cross-section of smaller PAH molecule, benzene (C_6H_6), and together with their own measurements of two larger PAH molecules, pyrene ($C_{16}H_{10}$) and coronene ($C_{24}H_{12}$), Verstraete et al. (1990) concluded that the photoionization cross-sections of large PAH molecules (e.g., 80 carbon atoms) are proportional to their number of carbon atoms. On the other hand, laboratory measurements of the recombination coefficients C_{rec} ($n_e C_{rec} = R_{rec}$, where n_e is the electron density) for $C_3H_3^+$, $C_5H_3^+$, $C_6H_6^+$, $C_7H_5^+$, and $C_{10}H_8^+$ show values ranging from 3×10^{-7} to 10×10^{-7} $cm^3 s^{-1}$ at 300 K, and indicate no correlation between the measured coefficients and the number of carbon atoms in the ion (Abouelaziz et al. 1993). This differs from past theoretical studies, which used classical electrostatics theory to adopt a coefficient that is proportional to the size of the PAH. For an interstellar PAH with 50 carbon atoms at 300 K, these earlier studies would adopt C_{rec} of about 1×10^{-5} $cm^3 s^{-1}$ in their ionization fraction calculations, which is about one to two orders of magnitude higher than those measured by Abouelaziz et al. (1993) for PAHs ≤ 10 carbon atoms. The lowest UV radiation field strength in our selected regions have $G_0 = 3$, and for a PAH of 50 carbon atoms R_{ion} is calculated as 3×10^{-8} s^{-1} (see Verstraete et al. 1990 for the calculations of R_{ion}). By adopting a $n_e = 10^{-2}$ cm^{-3} in the DIM (Omont 1986), we find from equation (3) that in order for PAHs to have $f(+) \geq 90\%$ (the mean value in figure 2c), C_{rec} should be less than 3.3×10^{-7} $cm^3 s^{-1}$. Our estimate of C_{rec} is by more than an order of magnitude lower than the theoretical calculations ($C_{rec} = 1 \times 10^{-5}$ $cm^3 s^{-1}$), but they are quite close to the measured values of Abouelaziz et al. (1993). If we adopt the theoretically calculated C_{rec} to estimate $f(+)$ in equation (3), we find that $f(+)$ is only 23% at $G_0 = 3$ and is 100% at $G_0 = 4500$. In this situation, the 11.2/7.7 μm band ratio will decrease from a value of 1.2 to 0.3 when the G_0 increase from 3 to 4500. Additional laboratory measurements of C_{rec} for larger PAHs (e.g., 50 to 100 carbon atoms) are definitely needed to make a better estimate of the ionization fraction of interstellar PAHs.

The above finding provides us useful information on the understanding of heating of the interstellar gas. Some studies have suggested that interstellar PAH molecules can be the dominant heating source of the interstellar H I gas if $\sim 10\%$ of the cosmic abundance of carbon is locked up in PAHs (d’Hendecourt & Léger 1987; Verstraete et al. 1990). In those studies the neutral PAHs absorb interstellar UV photons and their ejected photoelectrons heat up the surrounding interstellar gas. A large population of neutral PAHs is therefore required for maintaining the balance between heating and cooling rates. On the other hand, another study showed that the interstellar PAHs with sizes less than 100 carbon atoms contribute only a part to the heating of the diffuse interstellar gas, and that the major part is provided by PAHs clusters and small graphitic grains (Bakes & Tielens 1994). The present result suggests that interstellar PAHs cannot be the dominant source of heating of the diffuse interstellar gas unless their abundance is much larger than those adopted in the past studies.

Finally, the present finding of no systematic variation in the UIR band ratios in the DIM covering the central and disk regions of the Galaxy over a wide range of UV radiation field strengths

provides a new piece of information for the identification of the carriers of the UIR bands. In the PAHs model, the fitting of the observed UIR band emission in different astronomical environments requires a mixture of PAH molecules with different sizes and thermodynamical stability (Allamandola et al. 1999). Our finding suggests that the size distribution of the PAHs is the same in all locations and their thermodynamical stability is high. In the QCC and coal models, the enhancement of the 6.2, 7.7, and 8.6 μm bands has been attributed to oxidization (Sakata et al. 1987; Papoular et al. 1989). Therefore, the constant band ratio of 11.2/7.7 μm suggests that these species must be chemically stable in the DIM.

5. Summary

The major result of this paper is that there is no systematic variation in the UIR 6.2/7.7 μm , 8.6/7.7 μm , and 11.2/7.7 μm band ratios in the DIM covering the central and disk regions of the Galaxy over a wide range of UV radiation field strengths ($G_0 = 3$ to 4500). Comparing our results with the PAHs model: (1) the 6.2/7.7 μm band ratio suggests that PAHs in those environments have no systematic variation in their size distribution; (2) the 8.6/7.7 μm band ratio suggests that the degree of dehydrogenation of PAHs is independent of the strength of UV radiation field over a range of $G_0 = 3$ to 4500; and (3) the 11.2/7.7 μm band ratio suggests that the PAHs are mostly ionized in the DIM even though the UV radiation field strength is low. The last finding is incompatible with past theoretical studies, in which a large fraction of neutral PAHs is predicted in this kind of environment. Laboratory measurements of the recombination coefficients of large PAHs are needed to make a better estimate of the ionization fraction of interstellar PAHs. The finding that interstellar PAHs have very low abundance of neutral state molecules in the DIM does not support the suggestion that PAH molecules are the dominant source of heating of the diffuse interstellar gas by photoelectric emission. Finally, the present results imply that the carriers of the UIR bands have constant physical and chemical properties in the DIM, and this new information could help in the identification of the carriers.

The ISOPHOT data presented in this paper were reduced using PIA, which is a joint development by the ESA Astrophysics Division and the ISOPHOT Consortium with the collaboration of the Infrared Processing and Analysis Center (IPAC). Contributing ISOPHOT Consortium institutes are DIAS, RAL, AIP, MPIK, and MPIA. We are grateful to Louis Allamandola, Douglas Hudgins, and Jesse Bregman for helpful discussions about interstellar PAHs. We also thank IPAC for their help in the pointing reconstruction of the IRTS and the entire IRTS team for their efforts in ensuring the success of the IRTS mission. We also thank K. Kawara, Y. Satoh, and the Japanese ISO team for their continuous help and encouragement. We thank M. Burgdorf for the latest information on the LWS beam and the LWS IDT in Rutherford Appleton Laboratory, particularly S. Sidher, for the LWS data reduction. This work was performed while K. W. C. held a National Research Council-(NASA Ames Research Center) Research Associateship, and was supported by

NASA Grant 399-28-01. K. W. C is currently supported by the JSPS Postdoctoral Fellowship for Foreign Researchers. This work was supported in part by Grants-in-Aid for Scientific Research from JSPS.

REFERENCES

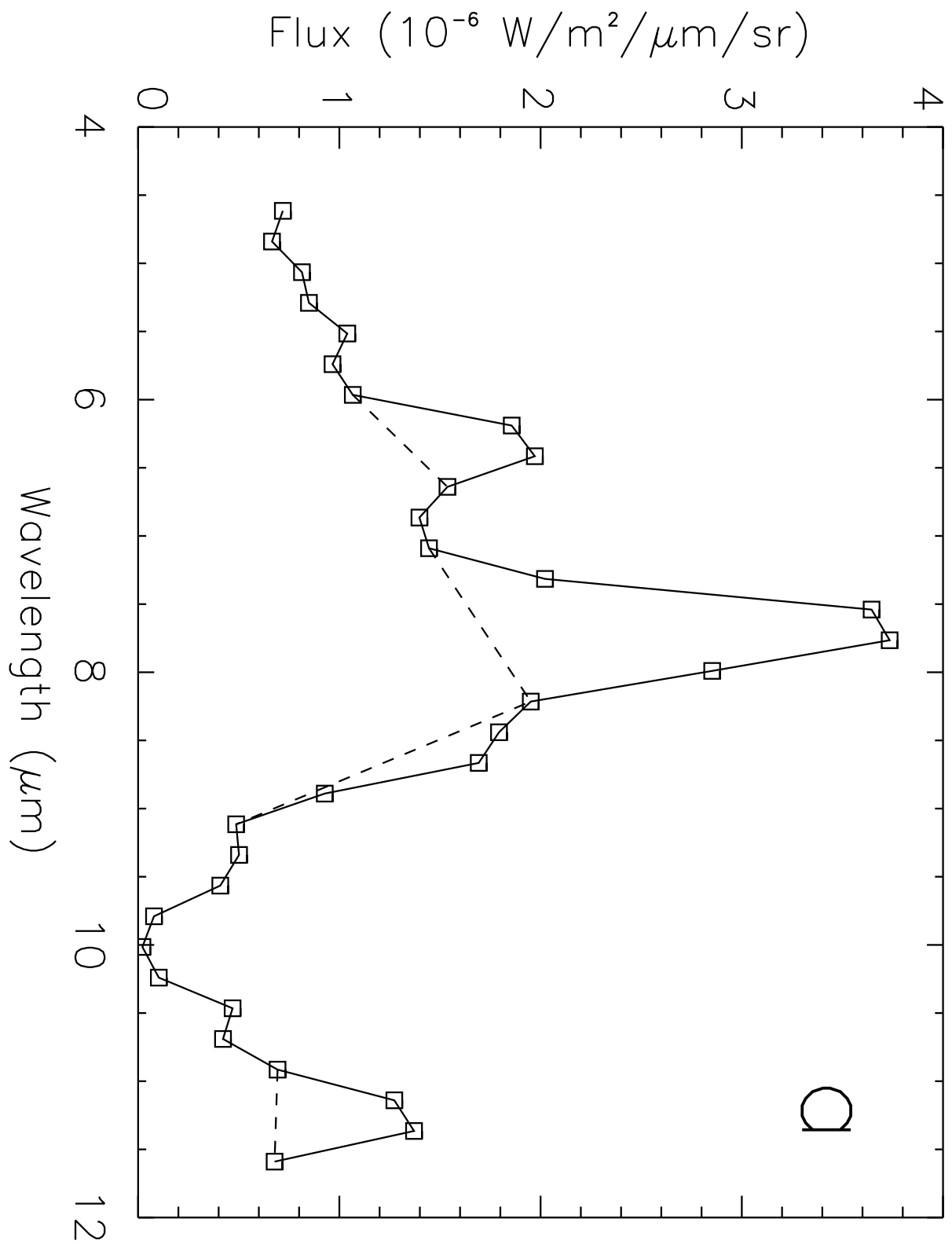
- Abouelaziz, H., Gomet, J. C., Pasquerault, D., Rowe, B. R., & Mitchell, J. B. A. 1993, *J. Chem. Phys.*, 99, 237
- Allamandola, L. J., Hudgins, D. M., & Sandford, S. A. 1999, *ApJ*, 511, L115
- Allamandola, L. J., Tielens, A. G. G. M., & Barker, J. R. 1989, *ApJS*, 71, 733
- . 1985, *ApJ*, 290, L25
- Bakes, E. L. O. & Tielens, A. G. G. M. 1994, *ApJ*, 427, 822
- Boulanger, F., et al. 1998, in *ASP Conf. Ser. 132, Star Formation with the Infrared Space Observatory*, ed. J. L. Yun & R. Liseau (San Francisco: ASP), 15
- Boulanger, F., Baud, B., & van Albada, G. D. 1985, *A&A*, 144, L9
- Bregman, J., Harker, D., Rank, D., & Temi, P. 1995, in *ASP Conf. Ser. 73, Airborne Astronomy Symposium on the Galactic Ecosystem: From Gas to Stars to Dust*, ed. M. R. Hass, J. A. Davidson, & E. F. Erickson (San Francisco: ASP), 63
- Bregman, J., Larson, K., Rank, D., & Temi, P. 1994, *ApJ*, 423, 326
- Burgdorf, M. et al., 1997, in *First ISO Workshop on Analytical Spectroscopy (ESA SP-419)*, 51
- Cesarsky, D., Lequeux, J., Abergel, A., Perault, M., Palazzi, E., Madden, S., & Tran, D. 1996, *A&A*, 315, L305
- Cohen, M., Allamandola, L., Tielens, A. G. G. M., Bregman, J., Simpson, J. P., Witteborn, F. C., Wooden, D., & Rank, D. 1986, *ApJ*, 302, 737
- Clegg, P. E. et al., 1996, *A&A*, 315, L38
- Dartois, E. & d’Hendecourt, L. 1997, *A&A*, 323, 534
- Draine, B. T. & Lee, H. M. 1984, *ApJ*, 285, 89
- Duley, W. W. & Williams, D. A. 1981, *MNRAS*, 196, 269
- Feinstein, A., Marraco, H. G., & Muzzio, J. C. 1973, *A&AS*, 12, 331
- Gillett, F. C., Forrest, W. J., & Merrill, K. M. 1973, *ApJ*, 183, 87

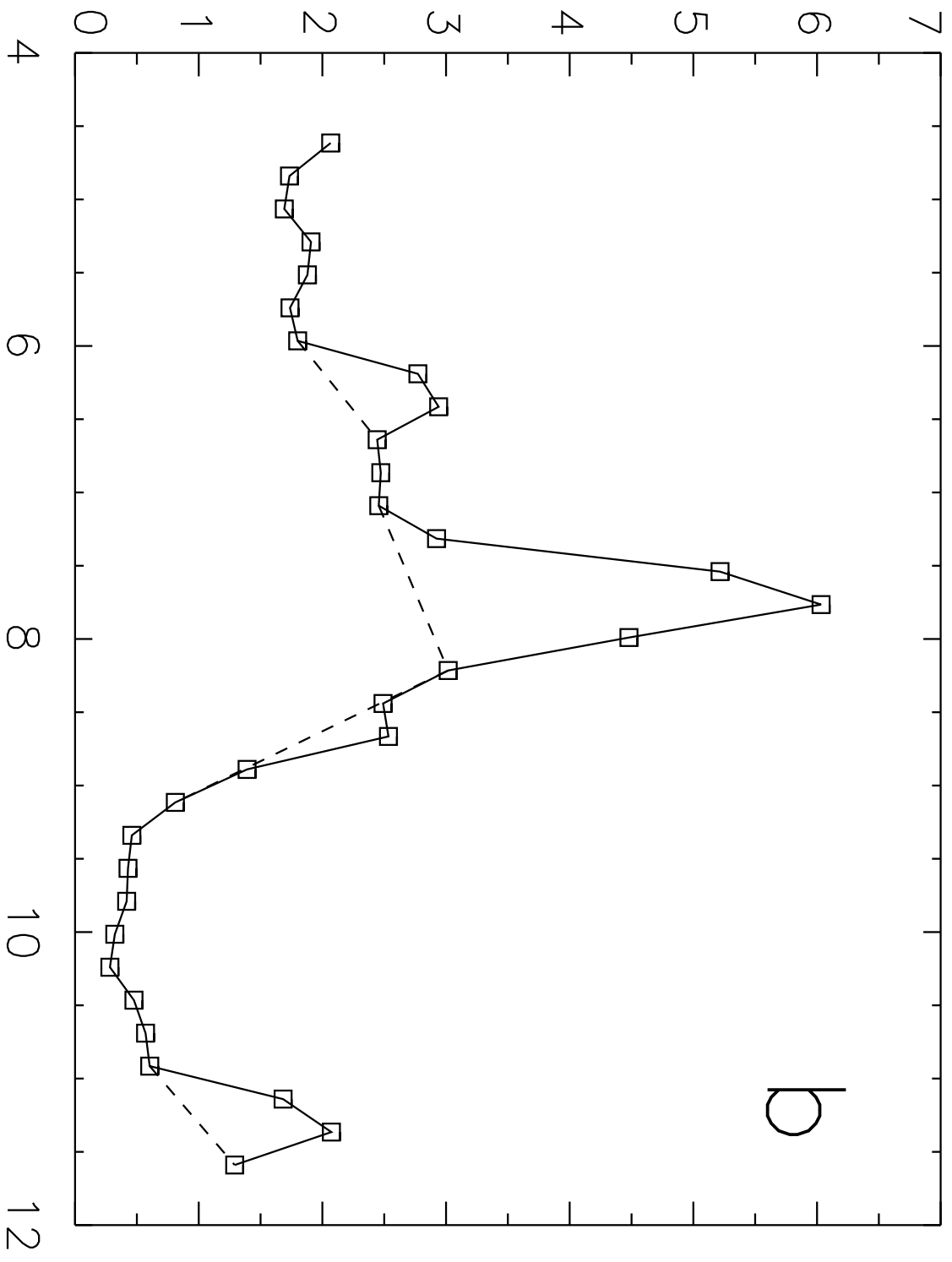
- Gry, C. 2000, The ISO Handbook, Volume IV: LWS - The Long-Wavelength Spectrometer
- Habing, H. J. 1968, Bull. Astr. Inst. Netherlands, 19, 421
- d'Hendecourt, L. B. & Léger, A. 1987, A&A, 180, L9
- Hudgins, D. M. & Allamandola, L. J. 1999, ApJ, 513, L69
- Joblin, C., Tielens, A. G. G. M., Geballe, T. R., & Wooden, D. H. 1996, ApJ, 460, L119
- Jourdain de Muizon, M., d'Hendecourt, L. B., & Geballe, T. R. 1990, A&A, 227, 526
- Kessler, M., et al. 1996, A&A, 315, L27
- Léger, A. & Puget, J. L. 1984, A&A, 137, L5
- Lemke, D., et al. 1996, A&A, 315, L64
- Lu, N. Y. 1998, ApJ, 498, L65
- Mathis, J. S. 1990, ARA&A, 28, 37
- Mattila, K., Lehtinen, K., & Lemke, D. 1999, A&A, 342, 643
- Mattila, K., Lemke, D., Haikala, L. K., Laureijs, R. J., Léger, A., Lehtinen, K., Leinert, Ch., & Mezger, P. G. 1996, A&A, 315, L353
- Murakami, H., et al. 1996, PASJ, 48, L41
- Mizutani, M., Onaka, T., & Shibai, H. 1999, in The Universe as seen by ISO, ed. P. Cox and M. F. Kessler (ESA SP-427), 719
- Okumura, K., Hiromoto, N., Shibai, H., Onaka, T., Makiuti, S., Matsuhara, H., Nakagawa, T., & Okuda, H. 1999, in Star Formation 1999, ed. T. Nakamoto, Nobeyama Radio Observatory, Japan, 96
- Okumura, K. 1998, Ph.D. thesis, Univ. of Tokyo
- Okumura, K., Hiromoto, N., Okuda, H., Shibai, H., Nakagawa, T., Makiuti, S., & Matsuhara, H. 1996, PASJ, 48, L123
- Omont, A. 1986, A&A, 164, 159
- Onaka, T., Yamamura, I., Tanabé, T., Roellig, T. L., & Yuen, L. 1996, PASJ, 48, L59
- Papoular, R., Conard, J., Giuliano, M., Kister, J., & Mille, G. 1989, A&A, 217, 204
- Puget, J. L., Léger, A., & Boulanger, F. 1985, A&A, 142, L19
- Roelfsema, P. R., et al. 1996, A&A, 315, L289

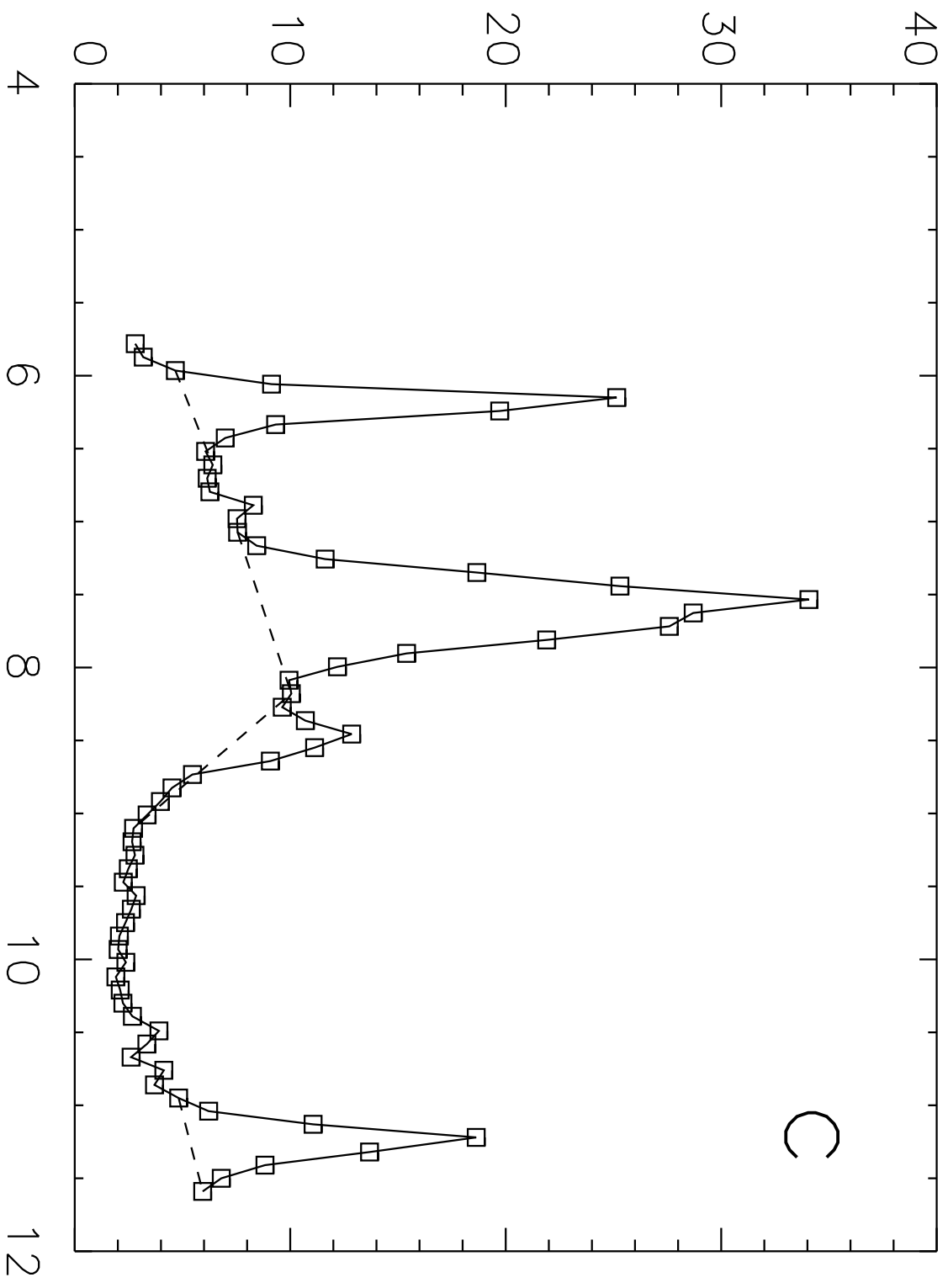
- Roellig, T. L., Onaka, T., McMahon, T. J., & Tanabé, T. 1994, *ApJ*, 428, 370
- Sakata, A., Wada, S., Onaka, T., & Tokunaga, A. T. 1987, *ApJ*, 320, L63
- Sakata, A., Wada, S., Tanabé, T., & Onaka, T. 1984, *ApJ*, 287, L51
- Schutte, W. A., Tielens, A. G. G. M., & Allamandola, L. J. 1993, *ApJ*, 415, 397
- Tanabé, T., Yamamura, I., Onaka, T., Chan, K.-W., Roellig, T. L., & Cohen, M. 1997, in *ASP Conf. Ser. 124, Diffuse Infrared Radiation and the IRTS*, ed. H. Okuda, T. Matsumoto, & T. L. Roellig (San Francisco: ASP), 25
- Tokunaga, A. T. 1997, in *ASP Conf. Ser. 124, Diffuse Infrared Radiation and the IRTS*, ed. H. Okuda, T. Matsumoto, & T. L. Roellig (San Francisco: ASP), 149
- Trams, N. et al., 1998, *ISOLWS Data Users Manual, Issue 5.0*
- Uchida, K. I., Sellgren, K., Werner, M. W., & Houdashelt, M. L. 2000, *ApJ*, 530, 817
- Verstraete, L., Léger, A., d’Hendecourt, L., Dutuit, O., & Défourneau, D. 1990, *A&A*, 237, 436
- Wheelock, S. L. et al. 1994, *IRAS Sky Survey Atlas Explanatory Supplement* (Publ. 94-11; Pasadena: JPL)

Fig. 1.— Samples of observed MIRS spectra at the (a) W51 ($l = 48^\circ.75$, $b = 0^\circ.00$) and (b) Galactic center ($l = -4^\circ.20$, $b = 0^\circ.13$) regions, and PHT-S spectra at the (c) Carina Nebula ($l = 287^\circ.305$, $b = -0^\circ.686$) region. The dashed lines show the continuum points used in the derivation of the UIR band ratios. In (c) the UIR bands are sharper than those in (a) and (b) and this is due to the high spectral resolutions of the PHT-S compared to those of the MIRS.

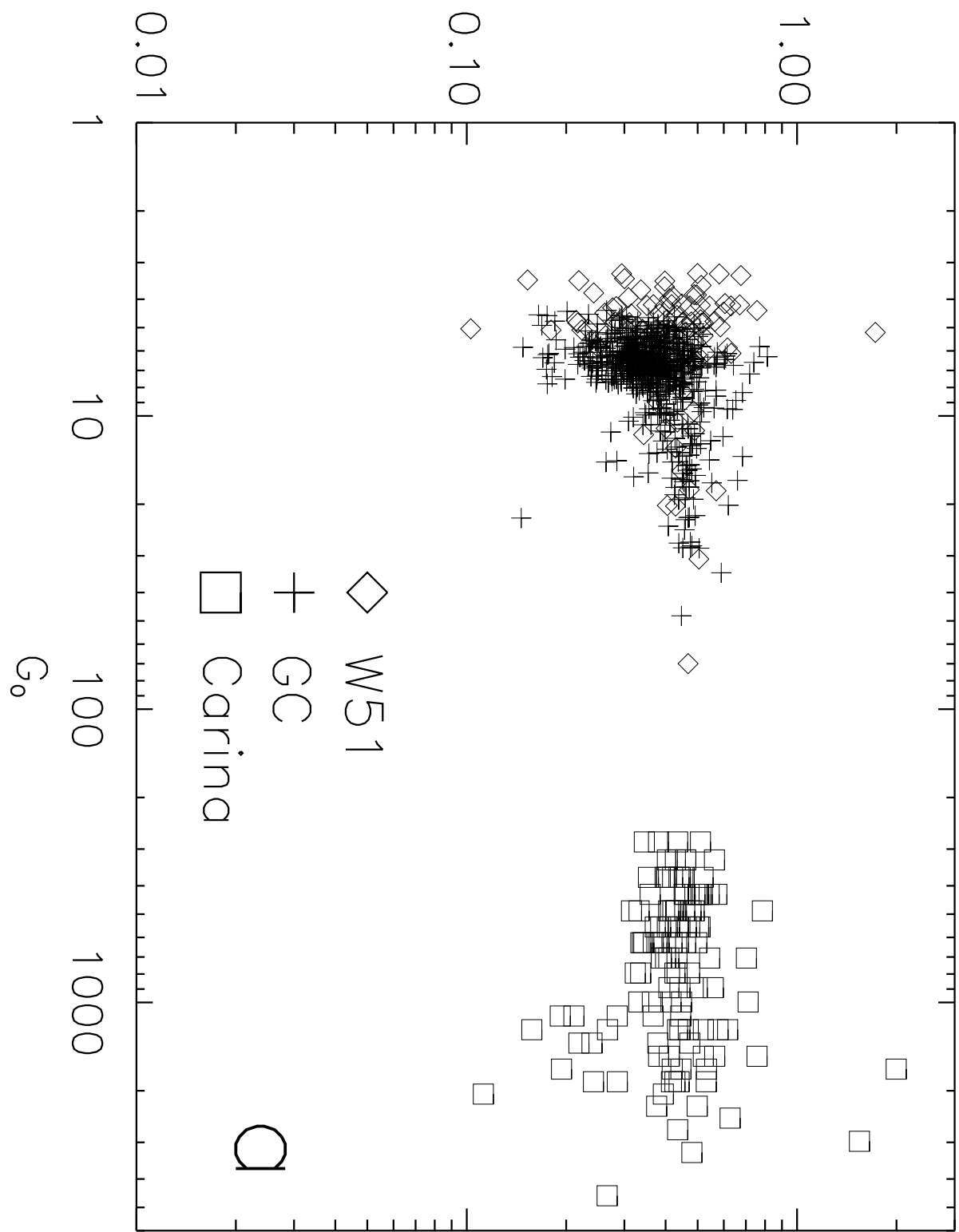
Fig. 2.— Relative band intensities of the UIR (a) $6.2/7.7 \mu\text{m}$, (b) $8.6/7.7 \mu\text{m}$, and (c) $11.2/7.7 \mu\text{m}$ vs. G_0 . The diamonds, plus symbols, and open squares are the data for the W51, Galactic center, and Carina Nebula regions, respectively. The scatter in the figures are largely due to statistical errors of the data, and the large scatter in (b) arises from the weak strength of the $8.6 \mu\text{m}$ band. In (c) the dashed lines at ratio of 0.3 and 1.5 mark the expected PAHs band ratio of 100% ionized and 100% neutral, respectively. See text for details of the derivation of these ratios.



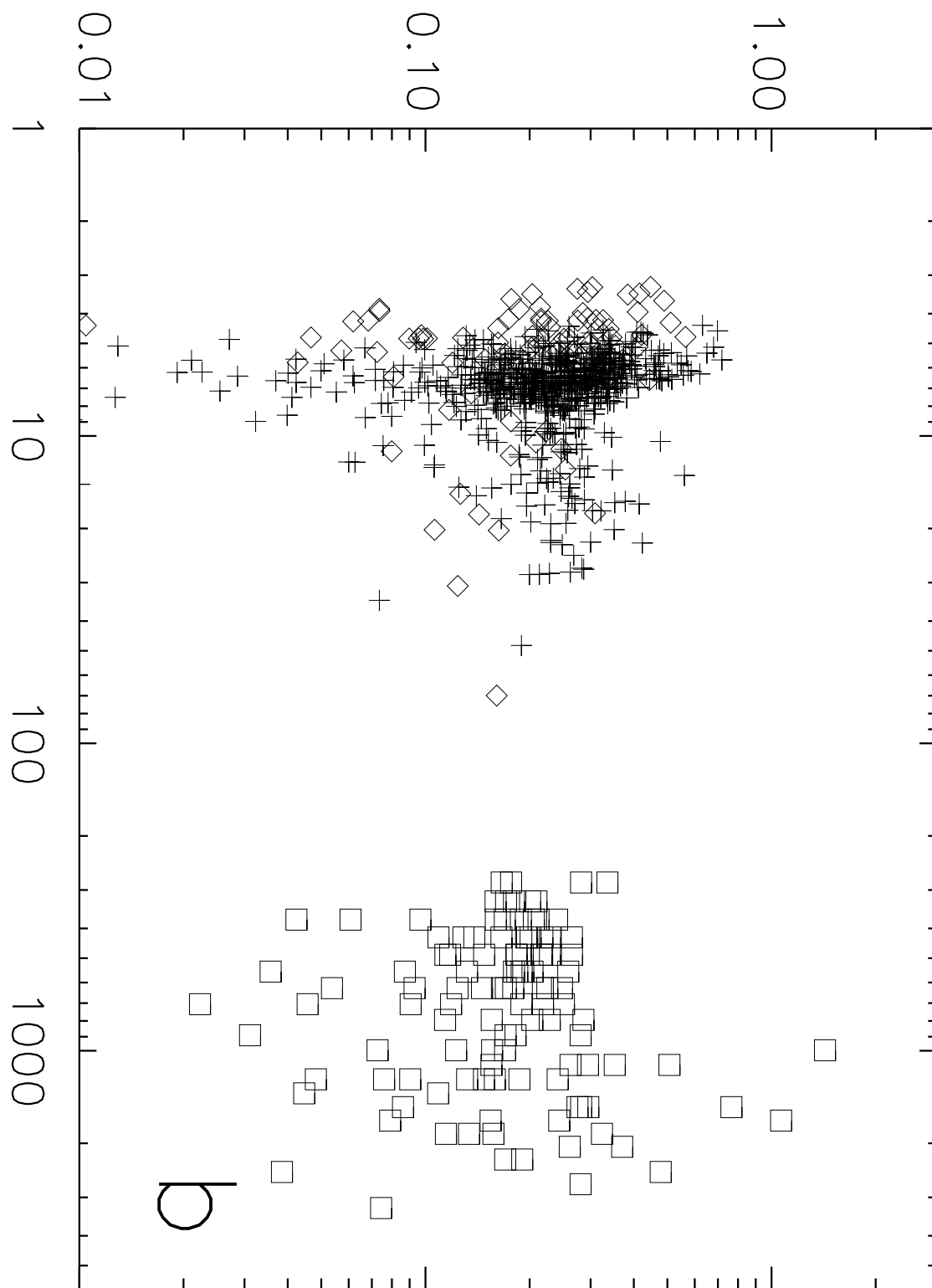




UIR 6.2/7.7 μm



UIR 8.6/7.7 μm



UIR 11.2/7.7 μm

